WTH3, which Encodes a Small G Protein, Is Differentially Regulated in Multidrug-Resistant and Sensitive MCF7 Cells

Kegui Tian,[1] Vladimir Jurukovski,[1] Liming Yuan,[2] Jidong Shan,[3] and Haopeng Xu[1]

[1]Department of Biochemistry and Cell Biology, State University of New York at Stony Brook, Stony Brook, New York; [2]North Shore-Long Island Jewish Research Institute, Manhasset, New York; and [3]Department of Molecular Genetics, Albert Einstein College of Medicine, Bronx, New York

Abstract

The *WTH3* gene's biological characteristics and relationship to multidrug resistance (MDR) were investigated further. Results showed that WTH3 was mainly located in the cytosol and capable of binding to GTP. In addition, *WTH3*'s promoter function was significantly attenuated in MDR (MFC7/AdrR) relative to non-MDR (MCF7/WT) cells. Advanced analyses indicated that two mechanisms could be involved in *WTH3*'s down-regulation: DNA methylation and *trans*-element modulations. It was found that the 5′ end portion of a CpG island in *WTH3*'s promoter was hypermethylated in MCF7/AdrR but not MCF7/WT cells, which could have a negative effect on the *WTH3* promoter. This idea was supported by the observation that a 45-bp sequence (DMR45) in this differentially methylated region positively influenced promoter activity. We also discovered that different nuclear proteins in MCF7/AdrR and MCF7/WT cells bound to methylated or nonmethylated DMR45. Moreover, a sequence containing a unique repeat that was also a positive *cis*-element for the promoter was attached by different transcription factors depending on whether they were prepared from MCF7/AdrR or MCF7/WT cells. These molecular changes, apparently induced by drug treatment, resulted in *WTH3*'s down regulation in MDR cells. Therefore, present studies support previous observations that *WTH3*, as a negative regulator, participates in MDR development in MCF7/AdrR cells. (Cancer Res 2005; 65(16): 7421-8)

Introduction

Multidrug resistance (MDR) often complicates the effectiveness of chemotherapeutic agents in treating various malignancies. Several MDR-related genes, such as *MDR1* and *MRP*, have been identified (1–4). Previously, we employed the methylation sensitive-representational difference analysis (MS-RDA) technique to study DNA hypermethylation events in MCF7/AdrR versus MCF7/WT, which led to the discovery of *WTH3* (5), a homologue of the *Rab6* and *Rab6c* genes that belong to the *ras* super family (6–10). *WTH3* encodes a 254-amino-acid (AA) polypeptide with 22 and 19 substitutions compared with Rab6 (8, 10) and Rab6c (7, 9), respectively. WTH3 also contains an elongated COOH terminus with no cysteine for posttranslational modification (geranylgeranylation), which indicated that it could have diverse biological uses compared with Rab6 (11, 12). Earlier studies found that *WTH3* was down-regulated in MDR cell lines, and introducing it into those lines reversed the MDR phenotype to various anticancer drugs (5). These findings suggested that *WTH3* could play an important role in MDR development.

To further understand *WTH3*'s biological functions, we recently examined the WTH3 protein's GTP binding activity and cellular location compared with Rab6c. Similar to Rab6c, WTH3 was capable of binding to GTP but displayed a notably different cellular distribution pattern. To comprehend its correlation with the MDR phenotype and the mechanisms influencing the down-regulation of *WTH3* in MDR cells, we examined the DNA methylation status (an epigenetic machinery for repressing gene expression in mammals; refs. 13–17) of the *WTH3* gene promoter in MCF7/AdrR and MCF7/WT cells and possible *cis*- and *trans*-element involvement. Thus, we found that differential DNA methylation, *cis*-responsible elements, and transcriptional factor modulation participated in manipulating *WTH3* gene expression in MDR versus non-MDR cells. Therefore, present studies supplied additional evidence to support the previous view that the *WTH3* gene functions as a negative regulator in MDR phenotype development in MCF7/AdrR cells.

Materials and Methods

Cell lines. MCF7/AdrR and MCF7/WT were grown under the conditions as described (5, 9).

Purification of GST/WTH3 and GST/Rab6c fusion proteins. To purify the GST/WTH3 fusion protein, sense (5′-CGGGATCCATGTCCGCGGGCGGAGACTTCG-3′) and antisense (5′-CGAATTCTAGCTAATAGATCATCTCCACG-3′) primers containing a *Bam*HI and *Eco*RI restriction site were used for PCR to amplify the coding region of *WTH3*. PCR fragments were cloned into the *Bam*HI and *Eco*RI sites of the pGEX vector (Amersham, Piscataway, NJ) to generate pGEX/WTH3. A sense (5′-CGGGATCCTCTAGTTCCACAATGTCC-3′) and antisense primer (5′-CGAATTCATGGAGATTAGCAGGAAC-3′) containing a *Bam*HI and *Eco*RI site were used to do PCR to obtain pGEX/Rab6c. The constructs and pGEX were transformed into *Escherichia coli*. Fusion protein inductions and purification were carried out as described (7). The protein purification was confirmed by SDS-PAGE gel and Western analysis using the glutathione *S*-transferase (GST) antibody (Santa Cruz Biotechnology, Santa Cruz, CA).

GTPγS binding assay. Five hundred nanograms of purified GST, GST/WTH3, and GST/Rab6c were tested for GTPγS binding ability. The experiments were done as previously described (7). Briefly, each sample was incubated with $\sim 1.5 \times 10^7$ cpm of [S^{35}]GTPγS in a binding buffer for 60 minutes. After terminating the reaction, the samples were filtered through nitrocellulose membranes and the amount of [S^{35}]GTPγS bound with each sample was measured in a scintillation counter. Nonspecific bindings were assayed with samples containing 0.1 mmol/L of unlabeled GTPγS. The experiments were done thrice.

Construction of *WTH3* and analysis of its cellular location in HeLa cells. The *WTH3* coding region was amplified by PCR where the sense primer (5′-GCAAGCTTCTAGTTCCACCATGTCCG-3′) and antisense primer (5′-CGGAATTCGCTTGTCAAGCTAATACTCC-3′) containing the *Hin*dIII and *Eco*RI site were used. PCR fragments of *WTH3* were cloned into

Requests for reprints: Haopeng Xu, Department of Biochemistry and Cell Biology, State University of New York at Stony Brook, R474 Life Science Building, Stony Brook, NY 11794-5215. Phone: 631-632-8566; Fax: 631-632-8575; E-mail: hduffy@notes.cc.sunysb.edu.

doi:10.1158/0008-5472.CAN-05-0658

corresponding sites of pEGFP-C1 (Clontech, Mountain View, CA) to generate pEGFP/WTH3. A sense (5′-CGGAATTCAATGTCCACGGGCGGAGAC-3′) and antisense primer (5′-CAGGATCCGGTTGAAGATGACATGGAG-3′) containing an *Eco*RI and *Bam*HI site were used for PCR to amplify *Rab6c* that was then cloned into pDsRed2-C1 (Clontech) to generate pDsRed/Rab6c. These constructs and the empty vector were transiently transfected, in parallel, into HeLa cells using the Lipofectamine Plus Transfection Kit (Invitrogen, Carlsbad, CA) following the manufacturer's instructions. After 24 hours, the cells were inspected under a confocal microscope.

Identification and isolation of the *WTH3* gene promoter. Information about the *WTH3* gene promoter was obtained from the NIH Genbank (accession nos. AF309646, AC079776, AC018865, AL136727, and BC044241). A sense (S-1) 5′-GGGGTACCCCGGTTTCTGACCTCTCACAGAGACG-3′ and antisense primer (AS-1) 5′-GAAGATCTTCGGTGGAACTAGAGGAGCTGTCG-3′ containing a *Kpn*I and *Bgl*II site were designed for PCR amplification. The PCR fragment covered a 679-bp fragment from position −679 to −1. Genomic DNA isolated from blood mononuclear cells of a healthy individual was used as a template for PCR using the GC-Rich PCR Amplification Kit (Roche, Indianapolis, IN) following the manufacturer's instructions. PCR fragments were cloned into the luciferase reporter plasmid, pGL3 (Promega, Madison, WI), to generate pGL/WTH3P. The amplified *WTH3* promoter in pGL/WTH3P was sequenced (Genewiz, Inc., North Brunswick, NJ).

Transient transfection and luciferase assays. pGL/WTH3P and pGL3 were transiently transfected into MCF7/WT to determine the *WTH3* promoter's activity. To explore whether the promoter was differentially regulated, pGL/WTH3P was transfected in parallel into MCF7/AdrR and MCF7/WT cells. In brief, 0.2 μg of the empty vector (negative control) or luciferase reporter construct was transfected along with 0.2 μg of pCMV/β-galactosidase when the cells (seeded onto 24-well plates) reached 50% to 70% confluence. After 24 hours, luciferase and β-galactosidase activity was measured using the Stady-Glo Luciferase Assay System and Beta-Glo Assay System (Promega) according to the manufacturer's instruction. Luciferase activities of transfectants were compared after normalizing their β-galactosidase activities and protein concentrations. The experiments were repeated four times.

Semiquantitative reverse transcription-PCR. Total RNAs were isolated from MCF7/AdrR and MCF7/WT cells by the High Pure RNA Isolation Kit (Roche). Semiquantitative reverse transcription-PCR was done using the Titan One tube RT-PCR system based on the manufacturer's protocol (Roche). The sense and antisense primers for *WTH3* were 5′-GATGGAACAATCGGGCTTCG-3′ and 5′-GCTGCTACACGTCGAAAGAGC-3′ (5). The sense and antisense primers for *MDR1* were 5′-CCTATCATTGCAATAGCAGG-3′ and 5′-GTTCAAACTTCTGCTCCTGA-3′. The sense and antisense primers for *β-actin* were 5′-GACGACATGGAGAAGATCTGG-3′ and 5′-ATCGGGCAGCTCGTAGCTCTTC-3′ (9). The length of the *WTH3, MDR1*, and *β-actin* PCR product was 341, 167, and 495 bp, respectively. PCR and quantification of PCR products were done as described (5, 9).

Genomic DNA purification and bisulfite genomic DNA sequencing assay. Genomic DNAs were isolated from MCF7/AdrR and MCF7/WT cells as described and treated with bisulfite using the CpG Genomic DNA Modification Kit (Chemicon, Temecula, CA) following the manufacturer's protocol. The treated DNAs were used as templates for PCR amplification. Two paired PCR primers were designed to cover the GC-rich region (−508 to 58) in the *WTH3* gene promoter. The sense and antisense sequences for the first paired primers (S/bis-1 and AS/bis-1) were 5′-GTTTTAGTTTTGGGAAGTTAAAG-3′ and 5′- CCAAAAACACCAACTTAAATTTCCTCAA-3′. The amplified sequence was from −306 to 58. The sense and antisense sequences for the second paired primers (S/bis-2 and AS/bis-2) were 5′-GTGTATTTAAAAAATTGTGTTGAGG-3′ and 5′-CCAAAAATATACTTTAACTTCCCAAAAC-3′. The amplified sequence was from −505 to −283. PCR amplification (50 μL) was done in a reaction containing 50 ng of bisulfite-treated DNA, 200 μmol/L of each deoxynucleoside, 3.5 mmol/L of $MgCl_2$, and 0.25 unit Taq Polymerase Gold. Conditions for doing 35 cycles of PCR were 94°C for 45 seconds, 55°C for 1 minute, and 72°C for 1 minute. PCR products were cloned into pGEM-TEasy (Promega) for transformation. Ten to 20 colonies derived from MCF7/AdrR or MCF7/WT were randomly picked and sequenced (Genewiz).

Electrophoretic mobility shift assay. Electrophoretic mobility shift assay (EMSA) was done using several probes to examine their binding patterns by the nuclear extracts prepared from MCF7/AdrR and MCF7/WT cells. Nuclear extracts were generated according to the method of Dignam et al. (18), and protein concentrations were determined by the Protein Assay Kit (Bio-Rad, Hercules, CA). Four probes were prepared for EMSA assays. Probes 1 and 2 covered the same region, −436 to −391, which was differentially methylated (the forward and reverse sequences were 5′-GCTGCGGCGGCGGCTGGGGAAGCCGAAGCGCCGCGCGTGAGA-3′ and 5′-TCTCACGCGCGGCGCTTCGGCTTCCCCAGCCGCCGCCGCCGCAGC-3′). The nine CpGs in probe 1 (DMR45) were not methylated, whereas those in probe 2 (mDMR45) were methylated with CpG methylase (NEB, Ipswich, MA). Successful methylation of probe 2 was confirmed by *Hha*I digestion, which recognizes the GCGC sequence but not $G^{m}CGC$. Probe 3 covered the sequence from −164 to −134 that only contained the full-length repeat (RR28; the forward and reverse sequences were 5′-GCCCTCCAGCCGGGCTCCTCCAGCCGGGCTCCTC-3′ and 5′-GAGGAGCCCGGCTGGAGGAGCCCGGCTGGAGGGC-3′). Probe 4 covered the sequence from −164 to −122 that included the repeat and putative Sp1 motif (RRSp1; the forward and reverse sequences were 5′-GCCCTCCAGCCGGGCTCCTCCAGCCGGGCTCCTCCACCGGCCC-3′ and 5′-GGGCCGGTGGAGGAGCCCGGCTGGAGGAGCCCGGCTGGAGGGC-3′). The probes were generated by annealing the forward and reverse oligonucleotides, followed by end-labeling using T4 polynucleotide kinase in the presence of [γ-^{32}P]dATP. To do EMSA, ~1 ng of the labeled probe was mixed with 5 μg of nuclear protein in a 20 μL binding buffer [25 mmol/L HEPES (pH 7.6), 50 mmol/L NaCl, 3 mmol/L $MgCl_2$, 25 mmol/L KCl, 1 mmol/L DTT, and 10% glycerol] containing 2 μg of poly(deoxyinosinic-deoxycytidylic acid). For competition experiments, 100-fold molar excess of unlabeled double strand probe was added into the reaction mix for 30 minutes at room temperature before the addition of the labeled probe. After incubation for 30 minutes, the reaction mixture was separated on a 4% nondenaturing-PAGE gel that was vacuum-dried and subjected to autoradiography using the STORM 840 PhosphorImager (Amersham). Super EMSA experiments were done in the presence or absence of 1 μg of nuclear factor-κB (NF-κB), WT1, or the Sp1 antibody (Santa Cruz Biotechnology) for 30 minutes and analyzed on a 4% nondenaturing-PAGE gel. For each probe, the experiments were repeated thrice.

Construction of the *WTH3* promoter with deletion mutants for luciferase assay. DMR45, RR14 (half of the repeat sequence), and RRSp1 were deleted from the original promoter sequence and constructed into pGL3 to create pGL/WTH3/DMR45^{-}, pGL/WTH3/RR14^{-}, and pGL/WTH3/RRSp1^{-}. To delete DMR45, an antisense primer (AS-2) 5′-CTCAGCAGGTTGG▼GATCCCGGATACATCTGC-3′, which represented the flanking sequences on both sides of DMR45, was paired with the S-1 primer to do the first round of PCR, where the pGL/WTH3P plasmid was used as a template. The same strategy was used to take out the RR14 and RRSp1 regions. To delete RR14, an antisense primer (AS-3) 5′-GGCCGGTGGAGG▼AGCCCGGCTGGAGGGCAGCA-3′, which represented the flanking sequences of a single repeat unit, was paired with the S-1 primer. To delete RRSp1, an antisense primer (AS-4) 5′-CTCTGCGCCCCTG▼-AGGGCTCGCCACAGACTGGC-3′, which represented the flanking sequences on both sides of the RRSp1 motif, was paired with the S-1 primer. The PCR product of each deletion mutant was gel purified and used as a sense primer that was paired with the antisense primer, AS-1, to do a second round of PCR. Conditions for this PCR were the same as the first round except that the annealing temperature was reduced to 40°C in the first five cycles. The resulting PCR fragments were cloned into pGL3. Success for creating the deletion mutants was confirmed by DNA sequencing. Activities of the mutated versus wild-type promoters in MCF7/WT and MCF7/AdrR were evaluated by luciferase assays as described. The experiments were done four times.

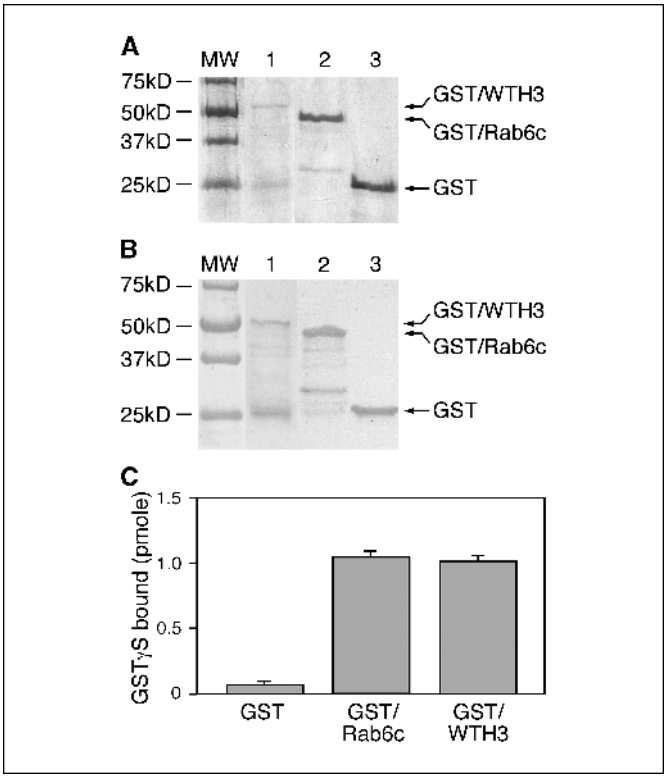

Figure 1. Results of WTH3 protein purification, Western blot, and [S^{35}]GTPγS binding assays. *A,* purified GST, GST/WTH3, and GST/Rab6c fusion proteins are displayed on a SDS-PAGE gel. *Lanes 1-3*, purified GST/WTH3, GST/Rab6c, and GST proteins (*arrows*). *B,* a duplicated SDS-PAGE gel was transferred onto a nylon membrane for Western analysis. The GST antibody recognizes GST/WTH3 in *lane 1*, GST/Rab6c in *lane 2*, and GST in *lane 3* (*arrows*). *C,* results of [S^{35}]GTPγS binding assays. *Columns,* GTPγS binding capacity for GST, GST/WTH3, and GST/Rab6c fusion proteins. Average of three independent experiments.

Results

GST, GST/WTH3, and GST/Rab6c fusion proteins were purified and the WTH3 protein was capable of binding to GTPγS. As we mentioned before, there are 19 substitutions in WTH3 relative to Rab6c. Some were located in the predicted GTP-binding domains (10). In addition, differing from most G protein, WTH3 does not possess any cysteine near its COOH terminus. Therefore, we were interested in determining whether or not WTH3 could bind to a GTP molecule. Consequently, constructs were generated where *WTH3* and *Rab6c* were linked to the *GST* gene. GST, GST/WTH3, and GST/Rab6c fusion proteins were expressed in *E. coli* and purified via affinity columns. Purification of the fusion proteins was confirmed on a SDS-PAGE gel (Fig. 1*A*). A duplicate gel was also transferred onto a nylon membrane for Western blot analysis where the GST protein antibody was used. Results showed that the fusion proteins and GST were purified (Fig. 1*B*).

To test whether the GST/WTH3 fusion protein could bind to GTP, GTPγS binding assays were done where the GST protein and GST/Rab6c fusion protein served as negative and positive controls, respectively. After incubating each protein with [S^{35}]GTPγS, we found that the GST protein bound with [S^{35}]GTPγS at an extremely low level suggesting a nonspecific binding event. However, GST/WTH3 and GST/Rab6c proteins showed similar binding capabilities with [S^{35}]GTPγS (Fig. 1*C*). When excessive amounts of unlabeled GTPγS were added into the reactions before the addition of [S^{35}]GTPγS, both WTH3 and Rab6c fusion proteins no longer bound to [S^{35}]GTPγS (data not shown). This information verified that the binding of the fusion proteins to [S^{35}]GTPγS was specific. Thus, our results showed that the 19 AA substitutions did not influence the *WTH3* gene product's GTP-binding activity.

WTH3 was mainly located in the cytoplasm of HeLa cells. Previously, the Echard group located the GFP-coupled Rab6c protein mainly on the membranes of the Golgi apparatus and *trans*-Golgi network (7). To determine *WTH3*'s protein location, pEGFP/WTH3 and the empty vector, pEGFP-C1 (control), were transfected into HeLa cells where the locations of WTH3 and enhanced green fluorescent protein (EGFP) were visualized under a confocal microscope. We found that most of the WTH3 protein was spread evenly in the cytoplasm and to a lesser extent inside the nuclei, whereas EGFP resided equally in both the cytoplasm and nuclei (Fig. 2). Identical results were observed when the *WTH3* gene was constructed into the pDsRed2-C1 vector where it was tagged with a red fluorescence protein (data not shown). In addition, the *Rab6c* gene was cloned into pDsRed2-C1 and introduced into HeLa cells where its location was found to be concentrated in the Golgi apparatus (Fig. 2).

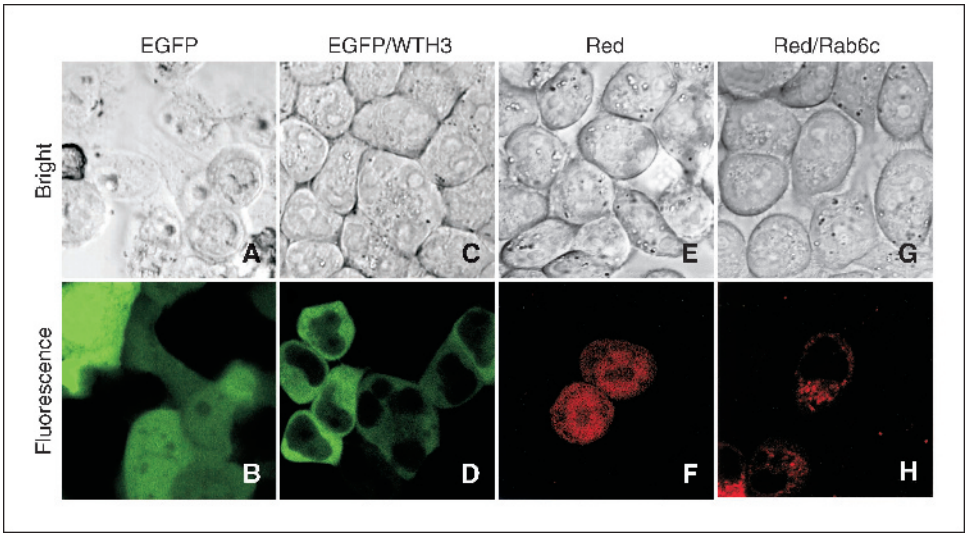

Figure 2. Confocal microscopy determined that WTH3 protein is located in the cytocol and nuclei of HeLa cells. pEGFP-C1 and pEGFP/WTH3 were transiently transfected into HeLa cells. *A* and *B,* bright and fluorescence field for cells transfected with pEGFP-C1. Fluorescence is generated by the cells containing the plasmid. *C* and *D,* bright and fluorescence field for cells transfected with pEGFP/WTH3. Fluorescence is generated by the cells containing the plasmid. *E* and *F,* bright and fluorescence field for cells transfected with pDsRed2-C1. *G* and *H,* bright and fluorescence field for cells transfected with pDsRed2/Rab6c.

The *WTH3* gene promoter was identified and cloned into pGL3. Information on the *WTH3* gene promoter region was obtained from the NIH Genbank. The *WTH3* promoter region contains an atypical TATA box and CAATT box at position −1197 and −1169 corresponding to the translation initiation site. In addition, TATA- or CAATT-like boxes are located at −616 and −576, respectively (Fig. 3*A*). We also found that there is a GC-rich zone that extends from −485 into the 5′-end coding region. The GC content is about 72% in the region from −485 to 1, which is also considered a CpG island because it includes 47 CpG sites (Fig. 3*A*). Using the Patch Search Program to look for potential consensus domains for existing transcription factors, we found that there is a putative Sp1 binding site (19, 20) located at the 3′ end of a 28-bp repeat sequence (−162 to −134). Putative NF-κB (21, 22) and WT1 (23, 24) domains are also identified in the region from −431 to −408. To test whether the upstream untranslated region contains promoter activity, a sequence (from −679 to −1) was generated by PCR and cloned into pGL3 to obtain pGL/WTH3P.

A 679-bp sequence in the *WTH3* gene's untranslated region contains promoter activity and was differentially regulated in MCF7/WT and MCF7/AdrR. The empty vector pGL3 or pGL/WTH3P, along with the pCMV/β-galactosidase plasmid that served as transfectional efficiency control, was transiently transfected in parallel into MCF7/WT cells. The promoter driven luciferase activity was measured as compared with the negative control. The result showed that a 679-bp sequence was able to transcribe the luciferase gene because the enzyme activity generated was about 60 times higher than that yielded by pGL3 (Fig. 4*A*). To understand the promoter's behavior in MDR cells, it was also introduced into MCF7/AdrR cells. We found that the *WTH3* gene promoter's capability to drive the reporter gene was reduced by >40% of that in MCF7/WT cells (Fig. 4*A*). This suggested that the *WTH3* gene was differentially regulated in those cells, which was consistent with the results obtained from measuring *WTH3* and *MDR1* expression levels. *WTH3* gene expression was low in MCF7/AdrR, but *MDR1* was reactivated, whereas it was high in MCF7/WT, where *MDR1* expression was undetected (Fig. 4*B-C*). These diversifications could be caused by drug treatment, which induced changes in *cis*- and/or *trans*-elements involved in the *WTH3* promoter's function. A reasonable candidate contributing to *cis*-element changes could be DNA methylation because the *WTH3* gene was discovered by the MS-RDA technique (5, 9, 25). Whereas changes related to *trans*-elements could be transcription factor variations. To test these hypotheses bisulfite genomic sequencing and EMSA assays were done.

A region (−481 to −305) in the *WTH3* promoter was hypermethylated in MCF7/AdrR but not MCF7/WT cells. Bisulfite genomic sequencing assays were done to examine the methylation patterns of CpGs in the GC-rich region that is ~500 bp in length (−485 to +22). Briefly, genomic DNAs were isolated from MCF7/AdrR and MCF7/WT cells and treated with bisulfite, which were then used as templates for PCR amplification to generate two DNA fragments that covered the GC-rich region. The resulting fragments were cloned into the vector. Ten to 20 inserts representing the upper and lower zones of the CpG island in both cell lines were randomly picked for sequencing. We found that the upper zone (−481 to −305) was differentially methylated. The GC content of

A

```
-679 aggtttctgacctctcacagagacggggagatagggacgttaaatttttataacatttctattta
-615 atatatatttaataatacataataaagtttttaaaatgtcaatttttgtccttttttctagtttgc
-551 attatttttgttttcaccgcaccattgtttttagtacatatgtttttgtgtatttaaaaaactgtg
-487 ttgaggcgccctgctcgccctgcgccagaggctcgcgcactcagcaggttggctgcggcggcg
-423 gcggctggggaagccgaagcgccgcgcgtgagagatcccggatacatctgcggtttgggctccg
-359 ccaccctccgtctctctcccgcaggtctctgagccgggtgcggaaggagggaacggccctagcc
-295 ttgggaagccaaagcacacccctggctcctgccgacaccgccctccttcccttcccagccgcgg
-231 gcctcgctccgtgctcggctactctgccgggaggcggcggcggctgccagtctgtggcgagccc
-167 tgctgcctccagccgggctcctccagccgggCTCCTCCACCGGCCCttgcaggggcgcagagg
-103 ctcggcgcccgcccttccgctcgccttttcgtcagccggctggaggagcatcggtccgggagg
 -39 tctctgggctgaggcggcgacagctcctctagttccaccatgtccgcgggcggagacttcggga
 +26 atccctgaggaaattcaagctggtgttcctgggggagc +63
```

B

#CpG*	MCF7/AdrR	MCF7/WT	#CpG	MCF7/AdrR	MCF7/WT	#CpG	MCF7/AdrR	MCF7/WT
1	1/10**	0/14	9	10/10	0/14	16	10/10	0/14
2	7/10	0/14	10	10/10	0/14	17	10/10	0/14
3	2/10	0/14	11	10/10	0/14	18	10/10	0/14
4	10/10	0/14	12	10/10	0/14	19	10/10	0/14
5	10/10	0/14	13	10/10	0/14	20	1/10	0/14
6	4/10	0/14	14	10/10	0/14	21	10/10	0/14
7	10/10	0/14	15	10/10	0/14	22	1/10	0/14
8	10/10	0/14						

* CpGs in the upper zone CpG island of the WTH3 gene promoter were numbered in bold type.

** Left and right numbers represent methylated CpGs and total colonies sequenced, respectively.

Figure 3. *A,* detailed information of the DNA sequence containing the functional *WTH3* gene promoter. TATA- and CCAAT-like boxes and the translational start codon were delineated by thin lined boxes. Primers used for bisulfite genomic DNA sequencing were marked in a gray-colored italic-formatted font. The CpG island involved in differential methylation was marked with bold type and the CpGs that were 100% methylated in MDR but not non-MDR cells were indicated with solid circles. CpGs that were partially methylated in the upper zone of CpG island were indicated with empty circles. Each differentially methylated CpG in the upper zone was numbered. Repeat sequence was underlined. Nucleotides with capital letters represent the putative Sp1 motif. The first letter of the start codon is counted as +1. Regions involved in deletion mutants were marked with thick lined boxes. *B,* methylation status of CpGs in the upper zone CpG island in the *WTH3* gene promoter.

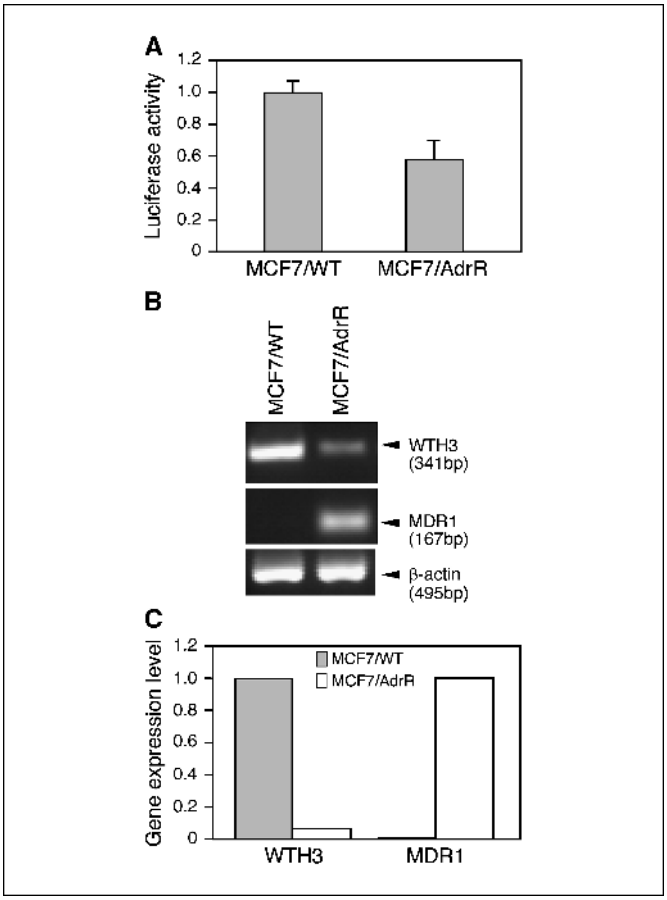

Figure 4. *A,* results obtained from luciferase assays show that the 679-bp sequence contains promoter activity and is differentially regulated in MCF7/WT and MCF7/AdrR cells. MCF7/WT and MCF7/AdrR cells were transiently transfected with pGL/WTH3P containing the *WTH3* gene promoter and promoter-free vector (pGL3). *Gray columns,* luciferase activities driven by the *WTH3* promoter in MCF7/WT and MCF7/AdrR cells, respectively. The activities were normalized with basal level enzymatic activities generated by the empty vector, protein concentrations, and transfection efficiencies. Average of four independent experiments. *B* and *C,* results obtained from measuring *WTH3* and *MDR1* expressions in MCF7 cell lines by SQRT-PCR. *B, arrows, WTH3, MDR1*, and *β-actin* PCR products generated from MCF7/WT and MCF7/AdrR. *C,* semiquantitative analyses of *WTH3* and *MDR1* expressions in MCF7/WT (*gray column*) versus MCF7/AdrR (*empty column*) cells, which were normalized with *β-actin* expressions.

this 176-bp region is about 75% and there are 22 CpGs. Among 10 sequenced clones derived from MCF7/AdrR, CpGs, 1, 2, 3, 6, 20, and 22, were methylated at a 10%, 70% 20%, 40%, 10%, and 10% rate, respectively, whereas the remaining 16 CpGs, which were located in the center of the region, were 100% methylated. However, none of the 22 CpG sites were methylated in MCF7/WT cells (Fig. 3*B*). These findings indicated that an epigenetic role was involved in regulating *WTH3* gene expression in MDR cells. Because methylated CpGs are potential targets for methyl-binding protein(s) (26–29) and other negative transcription factors (30–33), EMSA assays were done to test this possibility.

Different nuclear proteins in MCF7/WT and MCF7/AdrR were attracted to the methylated and nonmethylated probe. We chose the sequence encompassing −436 to −391 (DMR45) as the EMSA probe because it was very GC rich (~80% GC content) and contained nine CpGs that were all methylated in MDR but not in non-MDR cells (Fig. 3*A* and *B*). In addition, it also contained the putative WT1 and NF-κB motifs. To mimic an *in vivo* status, nonmethylated DMR45 in MCF7/WT (probe 1, or DMR45) and the methylated version in MCF7/AdrR (probe 2, or mDMR45) were prepared and their binding patterns with nuclear proteins in both cell lines examined. We found that the same two protein complexes in MCF7/WT bound to probe 1 or 2, whereas the other two protein complexes in MCF7/AdrR, which exhibited higher molecular weights than those in MCF7/WT, created identical binding patterns regardless of the probes' methylation status (Fig. 5*A*). We also noticed that the methylated probe attracted more proteins with higher molecular weight in both extracts. This observation was confirmed by densitometer analysis: both high molecular weight complexes in MCF7/WT and MCF7/AdrR bound to probe 2 about thrice more than those that bound to probe 1 (Fig. 5*A*). In addition, to verify if the probe included the predicted NF-κB and WT1 motifs, we did super EMSA using NF-κB and WT1 antibodies. The results showed that neither of the antibodies was able to shift the original binding patterns for each probe (data not shown).

Different proteins in MCF7/WT and MCF7/AdrR nuclear extracts bound to the repeat (RR28) and RR28 plus Sp1 motif (RRSp1). Whereas analyzing the *WTH3* promoter sequence, we uncovered a 28-bp repeat that consisted of two identical 14-bp sequences. In addition, its 3′ end was involved in a putative Sp1 motif (Fig. 3*A*). To determine whether this region played a role(s) in regulating *WTH3* during MDR development, probes 3 (RR28) and 4 (RRSp1) were prepared to do EMSA using nuclear extracts prepared from MCF7/AdrR and MCF7/WT. The information obtained for probe 3 showed that the binding patterns resulting from the two extracts were easily distinguished: two bands and a single band were generated by MCF7/WT and MCF7/AdrR extracts, respectively (Fig. 5*B*). As for probe 4, two bands were exhibited by MCF7/WT and three by MCF7/AdrR nuclear extracts (Fig. 5*B*). To test whether the Sp1 protein was among those binding proteins, super EMSA was done using the Sp1 antibody. The result showed that the Sp1 antibody was not able to shift any bands associated with the two extracts (data not shown).

At this moment we have discovered three *cis*-elements that could be responsible for the *WTH3* gene's down regulation in MDR cells. RR28 and RRSp1 were via association with their diverse *trans*-factors and DMR45 was through association with diverse *trans*-factors and differential methylation. To further understand whether those *cis*-elements influence *WTH3* promoter function, they were deleted from the original promoter.

The DMR45 and RR28 sequences had a positive influence on the *WTH3* promoter in MCF7/WT cells. To generate promoters without DMR45, a half of RR28 (RR14), or the RRSp1 sequence, a two-tier PCR technique was used. The resulting PCR fragments were cloned into pGL3 to obtain pGL/WTH3/DMR45^{-}, pGL/WTH3/RR14^{-}, and pGL/WTH3/RRSp1^{-} constructs. These constructs, pGL/WTH3P (positive control), the empty vector (negative control), and pCMV/β-galactosidase were transiently introduced into MCF7/WT cells. The enzyme activities driven by the mutated promoters were measured and compared with the normal promoter with justification of protein concentrations and transcription efficiency. The results showed that the activity of the promoter without the DMR45, RR14, or RRSp1 sequence was reduced >40% relative to the wild-type promoter (Fig. 6*A*). WTH3/RR14^{-} and WTH3/RRSp1^{-} displayed similar reduction. This indicated that RR28 and DMR45 played positive roles in the promoter's function in non-MDR cells.

The DMR45 and RR28 sequences no longer had a positive influence on the *WTH3* promoter in MCF7/AdrR cells. Because the EMSA results showed that different proteins originating from

MCF7/WT and MCF7/AdrR cells attached to DMR45, RR28, and RRSp1, we were interested in exploring the possible influences of those deletion mutants on the *WTH3* promoter in MCF7/AdrR cells. To do so, pGL/WTH3/DMR45^{-}, pGL/WTH3/RR14^{-}, and pGL/WTH3/RRSp1^{-} constructs were transfected into MCF7/AdrR cells. The luciferase activities driven by the mutated promoter were compared with that driven by the original promoter. The results showed that the modified promoters no longer played positive roles as they did in MCF7/WT cells. Instead, they produced slightly higher enzyme activities than the normal promoter (Fig. 6*A*). These disparities could be caused by interaction with different proteins. The deletions of RR14 and RRSp1 exhibited similar effects; thus, the Sp1 sequence exhibited no effect on the promoter. Detailed information for each construct in the two host lines is summarized in Fig. 6*B*.

Discussion

It is common knowledge that many changes happen in cells that develop MDR and multiple mechanisms may individually, or most likely synergistically, result in this phenotype (34–38). Unfortunately, many of them are presently unknown. By concentrating our efforts on understanding MDR, we discovered a MDR-related gene, *WTH3*, via the MS-RDA technique (5, 9, 25). The present studies provide further evidence that the *WTH3* gene could be an important component involved in MDR.

We first examined whether the *WTH3* gene product could bind to GTP like its homologues, Rab6 and Rab6c. Therefore, GST/WTH3 fusion proteins along with GST and GST/Rab6c were purified, and their capacity to bind to GTP evaluated. We found that WTH3 and Rab6c similarly bind to GTP confirming that the differences (the 19 substitutions and elongated tail lacking a consensus cysteine compared with Rab6c) in WTH3 do not influence its GTP binding ability. Second, we studied the cellular location of WTH3 using tagged EGFP fluorescence as markers. Differing from the Rab6c protein that was mainly located on the membranes of the Golgi apparatus and to a small amount on the ER (7), most of WTH3 was evenly spread in the cytosol, whereas some was also detected in the nuclei. The lack of a consensus cysteine at the COOH terminus of WTH3, whose role in many G proteins is to associate them to membranes after its fatty acylation, could cause this diversification. Thus, the *WTH3* gene's major biological pathway could be different from that associated with *Rab6c*.

Previous studies showed that there was a correlation between low expression of the *WTH3* gene and the MDR phenotype, and increasing its expression in MDR cells reversed the hosts' drug resistance to sensitivity (5). Therefore, understanding the mechanisms involved in the differential regulation of this gene in MDR and non-MDR cells is important. To do so, we identified the *WTH3* gene promoter. As with many other promoters, the promoter region contains an atypical TATA and CCAAT box, as well as a CpG island. Accordingly, we cloned a 679-bp part of the promoter region into pGL3 and its function in MCF7/WT cells was verified by luciferase assays. To see whether this promoter contained elements responsible for *WTH3*'s down-regulation in MDR cells, its activity was also measured in MCF7/AdrR cells. We found that the exogenous promoter functioned significantly stronger in non-MDR compared with MDR cells. Apparently, this result was consistent with earlier observations: endogenous *WTH3* gene expression in non-MDR cells was 4 to 15 times higher than that in MDR cells (5). Based on the existing information, several mechanisms could be involved in the *WTH3* promoter's down-regulation: differential DNA methylation and/or alteration of *trans*-elements.

To test these hypotheses, we first explored possible differential DNA methylation in the *WTH3* gene promoter in MDR versus non-MDR cells. DNA methylation is known to exert a negative effect on mammalian gene expression (13, 15, 39). For example, hypermethylation in the promoter regions of many recessive oncogenes is frequently reported (40–42), whereas demethylation of the *MDR1* promoter causes its reexpression in MDR cells (43–45). To determine the DNA methylation status of the *WTH3* promoter in MCF7/AdrR and MCF7/WT, bisulfite genomic sequencing assays were carried

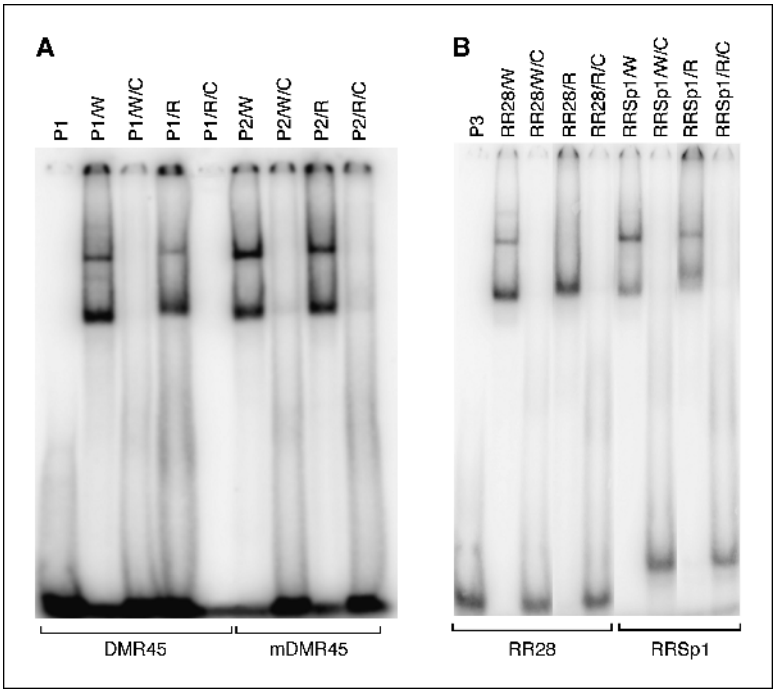

Figure 5. *A,* EMSA results when nonmethylated DMR45 (probe 1) and methylated DMR45 (mDMR45, or probe 2) probes were used. *Lane P1,* only the isotope labeled probe 1 that served as the negative control. *Lane P1/W,* labeled probe 1 and MCF7/WT nuclear extract. *Lane P1/W/C,* labeled probe 1, 100 times excess of cold probe 1 and MCF7/WT extract. *Lane P1/R,* labeled probe 1 and MCF7/AdrR extract, whereas P1/R/C contains labeled probe 1, 100 times excess of cold probe 1 and MCF7/AdrR nuclear extract. *Lane P2/W,* isotope labeled probe 2 and MCF7/WT nuclear extract. *Lane P2/W/C,* labeled 2 probe, 100 times excess cold probe 2 and MCF7/WT extract. *Lane P2/R,* labeled probe 2 and MCF7/AdrR extract. *Lane P2/R/C,* labeled probe 2, 100 times excess of cold probe 2 and MCF7/AdrR nuclear extract. The reactions were loaded on a 4% nondenaturing-PAGE gel. The experiments were repeated thrice. *B,* EMSA results when the RR28 (probe 3) and RRSp1 (probe 4) probes were used. *Lane P3,* only labeled probe 3 that served as negative control. *Lane RR28/W* and *RR28/W/C,* probe 3 was incubated with the MCF7/WT extract. *Lane RR28/W/C,* 100 times excess of cold probe 3. *Lane RR28/R* and *RR28/R/C,* probe 3 and MCF7/AdrR extract. *Lane RR28/R/C,* 100 times excess of cold probe 3. *Lane RRSp1/W* and *RRSp1/W/C,* probe 4 and MCF7/WT extract. *Lane RRSp1/W/C,* 100 times excess of cold probe 4. *Lane RRSp1/R* and *RRSp1/R/C,* probe 4 and MCF7/AdrR extract. *Lane RRSp1/R/C,* 100 times excess of cold probe 4. The samples were loaded on a 4% nondenaturing-PAGE gel. The experiments were repeated thrice.

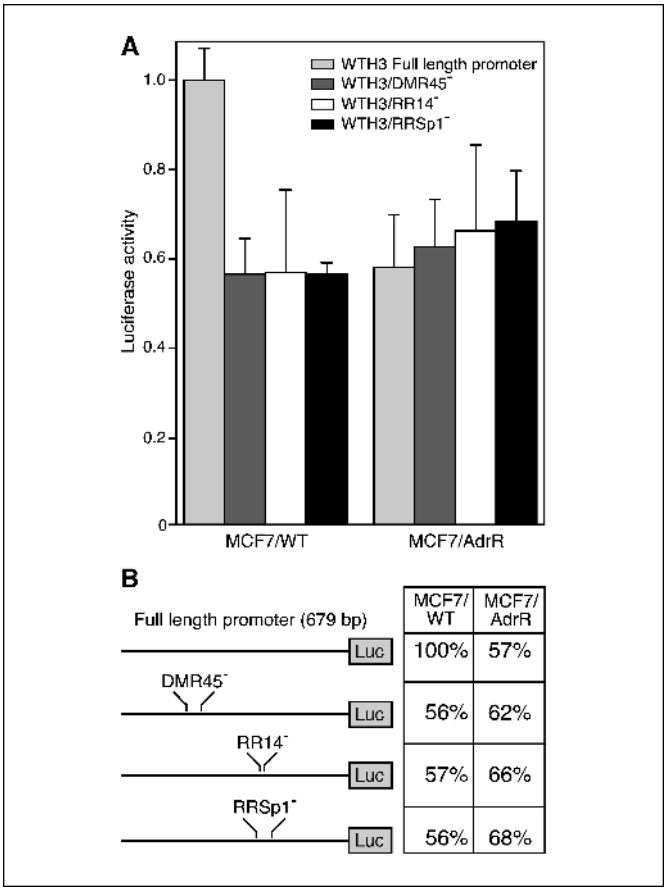

Figure 6. *A,* luciferase assay results for the *WTH3* promoter deletion mutants in MCF7/WT and MCF7/AdrR cells. *Gray column,* luciferase activity driven by the wild-type *WTH3* promoter. Enzyme activities driven by the mutated promoters where the DMR45 (*dark gray column*), RR14 (*empty column*), and RRSp1 (*black column*) were deleted. The host cells used were indicated under each section. The activities were normalized with the basal level enzymatic activities generated by the empty vector, protein concentrations, and transfection efficiencies. Averages of four independent experiments. *B,* detailed information of the wild-type *WTH3* promoter, its deletion constructs, and corresponding activities in two types of cells.

out. Consequently, the upper zone of the CpG island containing 22 CpGs was determined to be a differentially methylated region where six CpGs were partially methylated and the remaining 16 CpGs were fully methylated in the MDR genome. However, none of the 22 CpGs were methylated in the non-MDR genome. This discovery seemed consistent with the fact that *WTH3* was less expressed in MCF7/AdrR relative to MCF7/WT, which indicated that the *WTH3* promoter region's hypermethylation could be one of the mechanisms repressing the gene's transcription in MDR cells.

Accordingly, methylated CpGs could be potential targets for methyl-binding proteins and their copartners (26–33). Thus, we were interested in exploring whether any nuclear proteins could bind to the methylated *WTH3* promoter region. To do so, we prepared a probe, DMR45, which contained nine fully methylated CpGs in MDR cells, for EMSA assay. We found that two protein complexes in MCF7/AdrR cells bound to the methylated or nonmethyalted DMR45 probes. Because the binding patterns were the same, we assumed that those proteins were identical. In MCF7/WT cells, two protein complexes, with slightly lower molecular weights than those in MCF7/AdrR, bound to those probes. Based on the binding patterns, we believed that the proteins binding to both methylated and nonmethylated probes could also be the same. Due to the slight difference in molecular weights between the two sources, we do not know if the binding proteins prepared from MCF7/AdrR were modified versions of, or completely different from, those prepared from MCF7/WT. Because mDMR45 attracted thrice more proteins with higher molecular weight than DMR45, the quantitative variation related to DNA methylation could be a more significant factor with regard to the gene expression regulation. Furthermore, the binding proteins prepared from MDR and non-MDR cells bound to both methylated and nonmethylated probes. This suggests that they might not be known CpG-binding proteins, such as MeCP2, MBD1, and MBD2 (26–29), which only recognize methylated CpGs, and along with other corepressors, such as histone deacetylases, Sin3, histone methyltransferase, etc. (30–33) inhibit gene transcription. They are also not the dual protein, Kaiso, a zinc finger transcription factor recognizing the specific sequence and methyl-CpG dinucleotides (46, 47). This is because there is no Kaiso motif in the DMR45 probe.

Sequence analysis found the RR28 repeat sequence in the *WTH3* promoter. To explore this element's possible involvement in *WTH3* gene regulation, we first tested whether they were the targets of nuclear proteins. EMSA results using RR28 and RR28Sp1 as probes showed that they were targeted by different proteins in MCF7/AdrR and MCF7/WT cells, which suggested that drug treatment altered the *trans*-elements that could result in *WTH3*'s down-regulation in MDR cells. Thus far, DMR45, RR28, and RRSp1 could have potential roles in differentially regulating *WTH3* in those cell lines. To further understand their importance, they were deleted from the promoter and linked to the luciferase reporter gene. Luciferase activity analyses indicated that DMR45 and RR28 exhibited positive effects on the promoter in MCF7/WT cells. Therefore, the proteins binding to DMR45 and RR28 in those cells could be positive *trans*-factors. However, such positive effects were missing in MCF7/AdrR cells. This fundamental shift could be due to changes in the corresponding *trans*-factors induced by the drug. Instead, DMR45 and RR28 could interact with negative regulators.

In summary, current data indicates that *WTH3* encodes a G protein and is located in the cytoplasm. In addition, its promoter is differentially regulated in MDR cells via at least two mechanisms: differential DNA methylation and transcriptional factor modulation. Because deletion of DMR45 or RR28 only partially reduced the promoter's activity, hypermethylation of DMR45 or changing *trans*-factors of RR28 was not sufficient to explain the level of down regulation of *WTH3* expression in MCF7/AdrR cells. Therefore, additional regulatory *cis*- and/or *trans*-elements, as well as other mechanisms could be involved. A recent study indicated that the *WTH3* gene's copy number varies in the normal population and the authors raised a question of whether there is a relationship between its susceptibility and MDR (48). Clearly, studying *WTH3* gene function from different perspectives and molecular levels could elucidate its biological functions and pathway(s), which will lead to a better understanding of MDR development.

Acknowledgments

Received 2/24/2005; revised 5/13/2005; accepted 6/8/2005.

Grant support: Department of Defense Breast Cancer Research award DAMD17-00-1-0383 and American Cancer Society grant RSG-03-137-01-CDD.

The costs of publication of this article were defrayed in part by the payment of page charges. This article must therefore be hereby marked *advertisement* in accordance with 18 U.S.C. Section 1734 solely to indicate this fact.

We thank J.C. Duffy for preparation of the article.

References

1. Chen CJ, Chin JE, Ueda K, et al. Internal duplication and homology with bacterial transport proteins in the mdr1 (P-glycoprotein) gene from multidrug-resistant human cells. Cell 1986;47:381–9.
2. Cole SP, Bhardwaj G, Gerlach JH, et al. Overexpression of a Transporter gene in a multidrug-resistant human lung cancer cell line. Science 1992; 258:1650–4.
3. Gros P, Ben Neriah Y, Croop JM, Housman DE. Isolation and expression of a complementary DNA that confers multidrug resistance. Nature 1986;323:728–31.
4. Gros P, Croop J, Housman DE. Mammalian multidrug resistant gene: complete cDNA sequence indicates strong homology to bacterial transport proteins. Cell 1986;47:371–80.
5. Shan J, Yuan L, Budman DR, Xu H-P. WTH3, a new member of the Rab6 gene family, and multidrug resistance. Biochim Biophys Acta 2002;1589:112–23.
6. Echard A, Jollivet F, Martinez O, et al. Interaction of a Golgi-associated kinesin-like protein with Rab6. Science 1998;279:580–5.
7. Echard A, Opdam FJM, de Leeuw HJPC, et al. Alternative splicing of the human rab6A gene generates two close but functionally different isoforms. Mol Biol Cell 2000;11:3819–33.
8. Goud B, Zahroaui A, Tavitian A, Saraste J. Small GTP-binding protein associated with Golgi cisternae. Nature 1990;345:553–6.
9. Shan JD, Mason JM, Yuan L, et al. Rab6c, A new member of the Rab gene family, is involved in drug resistance in MCF7/AdrR cells. Gene 2000;257:67–75.
10. Zahraoui A, Touchot N, Chardin P, Tavitian A. The human Rab genes encode a family of GTP-binding proteins related to yeast YTP1 and SEC4 products involved in secretion. J Biol Chem 1989;264:12394–401.
11. Martinez O, Antony C, Pehau-Arnaudet G, Berger EG, Salamero J, Goud B. GTP-bound forms of rab6 induce the redistribution of Golgi proteins into the endoplasmic reticulum. Proc Natl Acad Sci U S A 1997;94:1828–33.
12. Martinez O, Schmidt A, Salamero J, Hoflack B, Roa M, Goud B. The small GTP-binding protein rab6 functions in intra-Golgi transport. J Cell Biol 1994;127:1575–88.
13. Antequera F, Bird PA. CpG islands in DNA methylation: molecular biology and biological significance. In: Jost JP, Saluz, HP, editors. Basel (Switzerland): Birkhauser Verlag; 1993. p. 169–85.
14. Antequera F, Bird AP. Number of CpG islands and genes in human and mouse. Proc Natl Acad Sci U S A 1993;90:11995–9.
15. Bird AP. CpG-rich islands and the function of DNA methylation. Nature 1986;321:209–13.
16. Doerfler W. DNA methylation and gene activity. Annu Rev Biochem 1983;52:93–124.
17. Kass SU, Pruss D, Wolffe AP. How does DNA methylation repress transcription? Trends Genet 1997; 13:444–9.
18. Dignam JD, Lebovitz RM, Roeder RG. Accurate transcription initiation by RNA polymerase II in a soluble extract from isolated mammalian nuclei. Nucleic Acids Res 1983;11:1475–89.
19. Benoist C, Chambon P. *In vivo* sequence requirements of the SV40 early promoter region. Nature 1981; 290:304–10.
20. Kadonaga JT, Carner KR, Masiarz FR, Tjian R. Isolation of cDNA encoding transcription factor Sp1 and function analysis of the DNA binding domain. Cell 1987;51:1079–90.
21. Beg AA, Sha WC, Bronson RT, Ghosh S, Baltimore D. Embryonic lethality and liver degeneration in mice lacking the RelA component of NF-κ B. Nature 1995; 376:167–70.
22. Zhou G, Kuo MT. NF-κB-mediated induction of mdr1b expression by insulin in rat hepatoma cells. J Biol Chem 1997;272:15174–83.
23. Rauscher FJ, Morris JF III, Tournay CE, et al. Binding of the Wilms' tumor locus zinc finger protein to the EGR-1 consensus sequence. Science 1990;250: 1259–62.
24. Reddy JC, Licht JD. The WT1 Wilms' tumor suppressor gene: how much do we really know? Biochim Biophys Acta 1996;1287:1–28.
25. Yuan LM, Shan JD, De Risi D, et al. Isolation of a novel gene, TSP50, by a hypomethylated DNA fragment in human breast cancer. Cancer Res 1999;59:3215–21.
26. Brackertz M, Boeke J, Zhang R, Renkawitz R. Two highly related p66 proteins comprise a new family of potent transcriptional repressors interacting with MBD2 and MBD3. J Biol Chem 2002;277:40958–66.
27. Feng Q, Zhang Y. The MeCP1 complex represses transcription through preferential binding, remodeling, and deacetylating methylated nucleosomes. Gene Dev 2001;15:827–32.
28. Meehan RR, Lewis JD, McKay S, Kleiner EL, Bird AP. Identification of a mammalian protein that binds specifically to DNA containing methylated CpGs. Cell 1989;58:499–507.
29. Nan X, Campoy FJ, Bird A. MeCP2 is a transcriptional repressor with abundant sites in genomic chromatin. Cell 1997;88:471–81.
30. Boeke J, Ammerpohl O, Kegel S, Moehren U, Renkawitz R. The minimal repression domain of MBD2b overlaps with the methyl-CpG-binding domain and binds directly to Sin3A. J Biol Chem 2000;275:34963–7.
31. Feng Q, Cao R, Xia L, Erdjument-Bromage H, Tempst P, Zhang Y. Identification and functional characterization of the p66/p68 components of the MeCP1 complex. Mol Cell Biol 2002;22:536–46.
32. Jones PL, Veenstra GJ, Wade PA, et al. Methylated DNA and MeCP2 recruit histone deacetylase to repress transcription. Nat Genet 1998;19:187–91.
33. Nan X, Ng HH, Johnson CA, et al. Transcriptional repression by the methyl-CpG-binding protein MeCP2 involves a histone deacetlyase complex. Nature 1998; 393:386–9.
34. Johnstone RW, Cretney E, Smyth MJ. P-glycoprotein protects leukemia cells against caspase-dependent, but not caspase-independent, cell death. Blood 1999;93: 1075–85.
35. Robinson LJ, Roberts WK, Ling TT, Lamming D, Sternberg SS, Roepe P. Human MDR1 protein overexpression delays the apoptotic cascade in Chinese hamster ovary fibroblasts. Biochemistry 1997;36: 11169–78.
36. Roepe PD, Wei L-Y, Cruz J, Carlson D. Lower electrical membrane potential and altered pHi homeostasis in multidrug-resistant (MDR) cells: further characterization of a series of MDR cell lines expressing different levels of p-gylcoprotein. Biochemistry 1993; 32:11042–56.
37. Simon SM, Schindler M. Cell biological mechanisms of multidrug resistance in tumors. Proc Natl Acad Sci U S A 1994;91:3497–504.
38. Smyth MJ, Krasovskis E, Sutton VR, Johnstone RW. The drug efflux protein, P-glycoptotein, additionally protects drug-resistant tumor cells from multiple forms of caspase-dependent apoptosis. Proc Natl Acad Sci U S A 1998;95:7024–9.
39. Siegfried Z, Cedar H. DNA methylation: a molecular lock. Curr Biol 1997;7:305–7.
40. Gonzalez-Zulueta M, Bender CM, Yang SA, et al. Methylation of the 5′ CpG island of the p16/CDKN2 tumor suppressor gene in normal and transformed human tissues correlates with gene silencing. Cancer Res 1995;55:4531–5.
41. Herman JG, Latif F, Weng Y, et al. Silenceing of the VHL tumor-suppressor gene by DNA methylation in renal carcinoma. Proc Natl Acad Sci U S A 1994;91: 9700–4.
42. Merlo A, Herman JG, Mao L, et al. 5′ CpG island methylation is associated with transcription silencing of the tumor suppressor p16/CDKN2/MTS1 in human cancers. Nat Med 1995;1:686–92.
43. Desiderato L, Davey MW, Piper AA. Demethylation of the human MDR1 5′ region accompanies activation of P-glycoprotein expression in a HL60 multidrug resistant subline. Somat Cell Mol Genet 1997;23:391–400.
44. El-Osta A, Kantharidis P, Zalcberg JR, Wolffe AP. Precipitous release of methyl-CpG binding protein 2 and histone deacetylase 1 from the methylated human multidrug resistance gene (MDR1) on activation. Mol Cell Biol 2002;22:1844–57.
45. Kusaba H, Nakayama M, Harada T, et al. Maintenance of hypomethylation status and preferential expression of exogenous human MDR1/PGY1 gene in mouse L cells by YAC mediated transfer. Somat Cell Mol Genet 1997;23:259–74.
46. Daniel JM, Reynolds AB. The catenin $p120^{ctn}$ interacts with Kaiso, a novel BTB/POZ domain zinc finger transcription factor. Mol Cell Biol 1999;19: 3614–23.
47. Prokhortchouk A, Hendrich B, Jorgensen H, et al. The p120 catenin partner Kaiso is a NDA methylation-dependent transcriptional repressor. Genes Dev 2001; 15:1613–8.
48. Sebat J, Lakshmi B, Troge J, et al. Large-scale copy number polymorphism in the human genome. Science 2004;305:525–8.